Published in final edited form as:
J Pharm Sci. 2009 August ; 98(8): 2611–2625. doi:10.1002/jps.21594.

HUMAN SKIN PERMEATION OF 3-O-ALKYL CARBAMATE PRODRUGS OF NALTREXONE

Haranath K. Vaddi[1,2], **Stan L. Banks**[1,3], **Jianhong Chen**[1,4], **Dana C. Hammell**[1], **Peter A. Crooks**[1], and **Audra L. Stinchcomb**[*,1]

[1]Department of Pharmaceutical Sciences, University of Kentucky College of Pharmacy, Lexington, Kentucky 40536-0082

Abstract

N-Monoalkyl and N,N-dialkyl carbamate prodrugs of naltrexone (NTX), an opioid antagonist, were synthesized and their *in vitro* permeation across human skin was determined. Relevant physicochemical properties were also determined. Most prodrugs exhibited lower melting points, lower aqueous solubilities, and higher oil solubilities than NTX. The flux values from N-monoalkyl carbamate prodrugs were significantly higher than those from NTX and N,N-dialkyl carbamates. The melting points of N-monoalkyl carbamate prodrugs were quite low compared to the N,N-dialkyl carbamate prodrugs and NTX. Heats of fusion for the N,N-dialkyl carbamate prodrugs were higher than that for NTX. N-Monoalkyl carbamate prodrugs had higher stratum corneum/vehicle partition coefficients than their N,N-dialkyl counterparts. Higher percent prodrug bioconversion to NTX in skin appeared to be related to increased skin flux. N,N-Dialkyl carbamate prodrugs were more stable in buffer and in plasma than N-monoalkyl carbamate prodrugs. In conclusion, N-monoalkyl carbamate prodrugs of NTX improved the systemic delivery of NTX across human skin *in vitro*. N,N-Dialkyl substitution in the prodrug moiety decreased skin permeation and plasma hydrolysis to the parent drug. The cross-sectional area of the carbamate head group was the major determinant of flux of the N-monoalkyl and N,N-dialkyl carbamate prodrugs of NTX.

Keywords

Naltrexone; carbamates; prodrugs; skin permeation; bioconversion; cross-sectional area

INTRODUCTION

Naltrexone (NTX), an opioid antagonist, is used for alcohol dependence and opioid addiction.[1,2] NTX hydrochloride is presently available as 50 mg oral tablets (ReVia®) in the United States. An oral dose of NTX undergoes extensive first pass metabolism (60-95%), and results in a lower percentage of active drug available for therapeutic effect.[3] Long-term usage of daily oral tablets is associated with non-compliance problems, and requires significant patient motivation in a traditionally difficult patient treatment population.[4,5] Additionally, oral NTX therapy is associated with gastrointestinal side effects, such as nausea, abdominal pain and vomiting.[6] Therefore, long-acting formulations that bypass first pass metabolism would be beneficial for NTX therapy. Transdermal drug delivery of NTX has the potential to obviate these problems by facilitating sustained action, therapeutic effect at lower drug dose, increased

*To whom correspondence should be addressed: astin2@email.uky.edu; Tel: 859-323-6192; FAX: 859-257-2787..
[2]Current address: Novartis, Lincoln, NE
[3]Current address: AllTranz Inc., Lexington, KY
[4]Current address: Clemson University, Clemson, SC

patient compliance, and minimal side effects. Transdermal therapy with NTX would also be very beneficial for already hepato-compromised alcohol and opioid addicts.

Since the skin is an excellent barrier against chemicals and toxins, only certain drugs with suitable physicochemical properties (such as low molecular weight and optimum lipophilicity), and a low daily therapeutic dose can successfully be formulated for transdermal delivery.[7] The NTX passive permeation rate across the skin does not achieve the required therapeutic plasma levels in humans due to the unsuitable physicochemical properties of the molecule.[8] However, drug permeation through skin can be enhanced by various methods, including prodrug design, chemical enhancers, and electrically-assisted methods, such as iontophoresis. Prodrugs are chemically modified inactive molecules that undergo bioconversion to the active drug in the body.[9] Prodrugs offer numerous potential advantages, such as targeted drug delivery, decreased toxic effects, improved drug stability, improved bioavailability, and improved organoleptic properties.[10-12] Prodrug delivery through the skin mirrors the toxicity profile of the parent drug, as long as the bioconversion of the prodrug to the parent drug in the skin is rapid. We previously reported the synthesis and human skin permeation of various 3-O-alkyl-carboxylate and 3-O-alkyl-carbonate prodrugs of NTX and obtained quantitative structure-permeability relationships.[13,14] Successful prodrugs for transdermal delivery should afford enhanced parent drug permeation, be readily bioconverted to parent drug, and should have sufficient chemical stability to withstand the rigors of formulation and storage. Carbamate prodrugs have been synthesized for a wide range of drug molecules in order to improve their therapeutic and physicochemical properties. Thus, carbamate prodrugs of norfloxacin were synthesized to mask its bitter taste and to increase its therapeutic efficacy[15]; of entacapone to improve oral bioavailability[16]; and of pseudomycins to decrease skin irritation potential.[17] Alexander *et al*.[18] synthesized carbamate prodrugs of β-blockers to enhance percutaneous transport, to reduce potential irritation in skin, and to improve ocular delivery. Carbamate prodrugs of the hydrophilic drugs, atenolol and pindolol, exhibited higher permeation compared to the parent drug through fuzzy rat skin *in vitro*, whereas prodrugs of lipophilic timolol and propranolol showed lower permeation compared to their parent drugs. Carbamate prodrugs have also been shown to combine improved chemical stability with rapid enzymatic hydrolysis.[16,19] The presence of a branched alkyl group in the carbamate prodrug moiety reportedly increases the chemical stability of the prodrug.[20] In the present study, we report the synthesis of N-monoalkyl and N,N-dialkyl 3-O-carbamate prodrugs of NTX and the results of human skin permeation studies evaluated *in vitro*. We also determined the physicochemical properties, chemical stability and plasma hydrolysis rates of these synthesized prodrugs in order to assess structure-permeability correlations.

MATERIALS AND METHODS

Materials

NTX base was purchased from Mallinckrodt Inc (St. Louis, MO). All prodrugs were synthesized from NTX free base. Hanks' balanced salts modified powder, sodium bicarbonate and light mineral oil were purchased from Sigma Chemical (St. Louis, MO). 4-(2-Hydroxyethyl)-1-piperazineethanesulfonic acid (HEPES), gentamicin sulfate, trifluroacetic acid (TFA), triethylamine (TEA), methanol, and acetonitrile (ACN) were obtained from Fisher Scientific (Fairlawn, NJ). 1-Octane sulfonic acid sodium salt was purchased from Chrom Tech® (Apple Valley, MN). All other chemicals and reagents used were analytical or HPLC grade.

Synthesis of Naltrexone Prodrugs

Ethyl naltrexone-3-O-carbamate—Ethyl isocyanate (170 mg, 2.34 mmol) and TEA (245 mg, 2.42 mmol) in dichloromethane (30 mL) were added to NTX (400 mg, 1.17 mmol). After

stirring at ambient temperature overnight under nitrogen, the reaction mixture was diluted with 100 mL of chloroform. The organic phase was washed with brine, dried over potassium carbonate, and concentrated on a rotary evaporator to afford the crude product as a brown oil. Purification by silica gel column chromatography (chloroform/methanol, 100/1) produced 200 mg (yield 41%) of the title compound as a white solid. An analytical sample was obtained by recrystallization from hexanes/ethyl alcohol. ^{1}HNMR ($CDCl_3$) δ 0.08-0.15 (2H, m), 0.48-0.58 (2H, m), 0.83 (1H, m), 1.15 (3H, m), 1.55-1.70 (2H, m), 1.85-1.90 (1H, m), 2.10-2.18 (1H, m), 2.25-2.45 (4H, m), 2.58-2.70 (2H, m), 3.00-3.15 (2H, m), 3.20-3.30 (3H, m), 4.75 (1H, s), 5.20 (1H, br s), 5.90 (1H, m), 6.66 (1H, m), 6.90 (1H, m) ppm. HRMS: calculated for $C_{23}H_{28}N_2O_5$ 412.1998, found 412.1995.

Propyl naltrexone-3-O-carbamate—Propyl isocyanate (823 mg, 9.57 mmol) and TEA (1.96 g, 19.2mmol) in dichloromethane (100 mL) were added to NTX (1.09 g, 3.20 mmol). After stirring at ambient temperature overnight under nitrogen, the reaction mixture was diluted with chloroform (150 mL). The organic phase was washed with brine, dried over potassium carbonate, and concentrated on a rotary evaporator to afford the crude product as a brown oil. Purification by silica gel column chromatography (chloroform/methanol, 100/1) produced 955 mg (yield 70%) of the title compound as a white solid. An analytical sample was obtained by recrystallization from hexanes/ethyl alcohol. ^{1}HNMR ($CDCl_3$) δ 0.12-0.18 (2H, m), 0.55-0.60 (2H, m), 0.82-0.98 (4H, m), 1.50-1.70 (4H, m), 1.90 (1H, m), 2.14 (1H, m), 2.30-2.45 (4H, m), 2.55-2.75 (2H, m), 2.95-3.10 (2H, m), 3.15-3.25 (3H, m), 4.70 (1H, s), 5.25 (1H, br s), 5.35 (1H, m), 6.65 (1H, m), 6.95 (1H, m) ppm. HRMS: calculated for $C_{24}H_{30}N_2O_5$ 426.2155, found 426.2110.

Butyl naltrexone-3-O-carbamate—Butyl isocyanate (200 mg, 1.97 mmol) and TEA (240 mg, 2.37 mmol) in dichloromethane (100 mL) were added to NTX (615 mg, 1.80 mmol). After stirring at ambient temperature overnight under nitrogen, the reaction mixture was diluted with chloroform (150 mL). The organic phase was washed with brine, dried over potassium carbonate, and concentrated on a rotary evaporator to afford the crude product as a brown oil. Purification by silica gel column chromatography (chloroform/methanol, 100/1) produced 420 mg (yield 53%) of the title compound as a white solid. An analytical sample was obtained by recrystallization from hexanes/ethyl alcohol. ^{1}HNMR ($CDCl_3$) δ 0.10-0.18 (2H, m), 0.55-0.58 (2H, m), 0.80-0.95 (4H, m), 1.30-1.42 (2H, m), 1.55-1.70 (4H, m), 1.90 (1H, m), 2.14 (1H, m), 2.30-2.45 (4H, m), 2.55-2.75 (2H, m), 3.00-3.15 (2H, m), 3.18-3.30 (3H, m), 4.70 (1H, s), 5.25 (1H, br s), 5.50 (1H, m), 6.63 (1H, m), 6.95 (1H, m) ppm. HRMS: calculated for $C_{25}H_{32}N_2O_5$ 440.2311, found 440.2317.

Pentyl naltrexone-3-O-carbamate—n-Pentyl isocyanate (235 mg, 2.04 mmol) and TEA (80 mg, 0.79 mmol) in dichloromethane (100 mL) were added to NTX (694 mg, 2.04 mmol). After stirring at ambient temperature overnight under nitrogen, the reaction mixture was diluted with chloroform (150 mL). The organic phase was washed with brine, dried over potassium carbonate, and concentrated on a rotary evaporator to afford the crude product as a brown oil. Purification by silica gel column chromatography (chloroform/methanol, 100/1) produced 603 mg (yield 65%) of the title compound as a white solid. An analytical sample was obtained by recrystallization from hexanes/ethyl alcohol. ^{1}HNMR ($CDCl_3$) δ 0.15-0.18 (2H, m), 0.50-0.60 (2H, m), 0.80-0.95 (4H, m), 1.25-1.35 (4H, m), 1.50-1.70 (4H, m), 1.90 (1H, m), 2.15 (1H, m), 2.30-2.45 (m, 4H), 2.55-2.70 (2H, m), 2.95-3.10 (2H, m), 3.18-3.30 (3H, m), 4.70 (1H, s), 5.20 (1H, br s), 5.50 (1H, m), 6.65 (1H, m), 6.90 (1H, m) ppm. HRMS: calculated for $C_{26}H_{34}N_2O_5$ 454.2468, found 454.2485.

N,N-dimethyl naltrexone-3-O-carbamate—A mixture of NTX (240 mg, 0.70 mmol) and TEA (100 μL, 0.70 mmol) in 20 mL of anhydrous methylene chloride were cooled to 0°C in

an icebath. To this stirred mixture was added N,N-dimethylcarbamoyl chloride (0.80 mmol). After stirring for 10 h, the resulting reaction mixture was diluted with methylene chloride (40 mL) and washed with 10% aqueous sodium carbonate (2 × 40 mL) and then water (40 mL). The organic solution was separated and dried over anhydrous potassium carbonate and reduced to a small volume under reduced pressure. The desired product was precipitated by trituration with excess pentane. The resulting solid was filtered, washed with cold pentane and air-dried to provide a white powder. ^{1}HNMR ($CDCl_3$): δ 0.15 (2H, m), 0.56 (2H, m), 0.88 (1H, m), 1.56-1.70 (2H, m), 1.88 (1H, m), 2.15 (1H, m), 2.32 (1H, m), 2.37-2.50 (3H, m), 2.54-2.76 (2H, m), 2.92-3.16 (5H, m), 3.12 (3H, s), 3.21(1H, d, J = 5.7Hz), 4.71 (1H, s), 5.23 (1H, br s), 6.66 (1H, d, J = 8.1Hz), 6.86 (1H, d, J = 8.1Hz) ppm. MS (LC-MS electrospray), M^+ = 412 m/z.

N,N-diethyl naltrexone-3-O-carbamate—The diethyl carbamate prodrug was prepared using the same procedure as described for the preparation of the N,N-dimethyl carbamate prodrug utilizing N,N-diethylcarbamoyl chloride in place of N,N-dimethylcarbamoyl chloride. ^{1}HNMR ($CDCl_3$): δ 0.16 (2H, m), 0.55 (2H, m), 0.88 (1H, m), 1.12-1.35 (6H, m), 1.55-1.71 (2H, m), 1.89 (1H, m), 2.15 (1H, m), 2.35-2.50 (3H, m), 2.52-2.75 (2H, m), 2.92-3.15 (2H, m), 3.21 (1H, d, J = 5.7Hz), 3.25-3.55 (4H, m), 4.71 (1H, s), 5.23 (1H, br s), 6.66 (1H, d, J = 8.1Hz), 6.86 (1H, d, J = 8.1Hz) ppm. MS (LC-MS electrospray), M^+ = 440 m/z.

N,N-diisopropyl naltrexone-3-O-carbamate—Triphosgene (2.82 g, 9.4 mmol) was added to diisopropylamine (480 mg, 4.70 mmol) and TEA (3.8 g, 37.6 mmol) in dichloromethane (100 mL). The reaction mixture was stirred for two hours in an ice-water bath. NTX (800 mg, 2.34 mmol) was added, and the reaction mixture was stirred at ambient temperature overnight under nitrogen. The reaction mixture was diluted with chloroform (150 mL), the organic phase was washed with brine, dried over potassium carbonate, and concentrated on a rotary evaporator to afford the crude product as a brown oil. Purification by silica gel column chromatography (chloroform/methanol, 100/1) produced 548 mg (yield 50%) of the title compound as a white solid. An analytical sample was obtained by recrystallization from hexanes/ethyl alcohol. ^{1}HNMR (DMSO-d_6) δ 0.10-0.18 (2H, m), 0.45-0.55 (2H, m), 0.87 (1H, m), 1.05- 1.50 (8H, m), 1.78 (1H, m), 1.95-2.15 (2H, m), 2.30-2.45 (3H, m), 2.55-2.70 (2H, m), 2.85-2.98 (1H, m), 3.05-3.20 (2H, m), 3.25-3.40 (8H, m), 4.90 (1H, m), 5.15 (1H, br s), 6.70 (1H, m), 6.85 (1H, m) ppm. HRMS: calculated for $C_{27}H_{36}N_2O_5$ 468.2626, found 468.2641.

HPLC Analysis

A modification of the high-pressure liquid chromatography (HPLC) assay described by Hussain *et al*. [11] was used for the analysis of NTX and its prodrugs. The HPLC system consisted of a Waters (Waters Corp., Milford, MA) 717 plus Autosampler, a Waters 1525 Binary HPLC Pump and a Waters 2487 Dual Wavelength Absorbance Detector with Waters Breeze software. A Brownlee C-18 reversed-phase Spheri-5 μm column (220 × 4.6 mm) with a C-18 reversed phase 7 μm guard column (15 × 3.2 mm) was used with the UV detector set at a wavelength of 215 nm. The mobile phase comprised of 70:30 ACN:0.1% TFA with 0.065% 1-octane sulfonic acid, adjusted to pH 3.0 with TEA. The flow rate of the mobile phase was 1.5 mL/min and 100 μL of sample volume was injected onto the column. Diffusion samples were analyzed with a set of external standards, and exhibited excellent linearity over the entire concentration range employed in the assays.

The drugs were extracted from the buffer samples by solid phase extraction (30 mg 1cc Oasis® HLB, Waters Corp., Milford, MA). Before loading the aqueous drug samples (5 mL), the cartridges were conditioned with 1 mL of methanol and 1 mL of purified water. After loading

the samples, the cartridges were washed with 1 mL of 5% methanol and the drug was eluted with ACN and analyzed by HPLC.

Differential Scanning Calorimetry of NTX and NTX Prodrugs

Differential scanning calorimetry (TA Instruments 2920) was carried out for NTX and its carbamate prodrugs to determine their respective melting points. An accurately weighed sample of drug (2-5 mg) was sealed into aluminum pans and thermograms were recorded at increments of 10°C/min from ambient temperature to 250°C. Measurements were repeated once for a total of two scans on NTX and the NTX prodrugs. Since endothermic peaks were not detected for the very low-melting N-monoalkyl carbamate prodrugs on this instrument, melting points of these drugs were determined on a Fischer-Johns melting point apparatus.

Solubility

The solubilities of NTX and the carbamate prodrugs were determined by adding an excess quantity of the test drug/prodrug to mineral oil or pH 7.4 HEPES-buffered Hanks' balanced salts solution at 32°C. Equilibration of the solutions was achieved on a shaking water bath for 8 h. Since the N-monosubstituted carbamate prodrugs were found to be less stable in this buffer, their solubility was determined after sonicating excess solid in the buffer at 32°C for 15 min. The buffer solubility of NTX was also determined under these conditions and found to be equivalent to the 8 h solubility measurement. After equilibration, samples were withdrawn into a pre-warmed glass syringe, filtered through a syringe filter, discarding the first 30% of the initial filtrate (Mineral oil: Millex FG-13 filter, Millipore and buffer: nylon filter, Gelman), measured with respect to volume (10 μL), and diluted with ACN or Hanks' buffer. The buffer samples were immediately extracted by solid phase extraction into ACN. All samples were analyzed by HPLC.

In Vitro Skin Diffusion Studies

Human skin harvested during abdominoplasty was used for the diffusion studies. Skin sections were obtained by using a Padgett Instruments® dermatome set to 250 microns and stored at ×20°C. A PermeGear flow-through (In-Line, Riegelsville, PA) diffusion cell system was used for the skin permeation studies. Trans-epidermal water loss was measured (Evaporimeter EP1™, ServoMed, Sweden) after securing the skin in the cells. Skin samples with readings below 13 $g/m^2/h$ were used for the diffusion studies. Diffusion cells were kept at 32°C with a circulating water bath. Data was collected by using human skin from a single donor with three cells for NTX and three to four cells for the NTX prodrugs. Due to high intersubject human skin permeation variability, the prodrug permeation was compared against NTX permeation for each individual donor skin sample. The receiver solution was HEPES-buffered Hanks' balanced salts with gentamicin at pH 7.4, and the flow rate was adjusted to 1.1 mL/h. An excess quantity of NTX or NTX prodrug was added to light mineral oil and the mixture was sonicated for 10 min and then applied onto the skin. An excess quantity of the drug was used in the donor compartment throughout the diffusion experiment in order to maintain maximum and constant chemical potential of the drug in mineral oil. Each cell was charged with 0.25 mL of the respective drug suspension. Samples were collected in six-hour increments over 48 h. All samples were stored at 4°C until processed by solid phase extraction. Human tissue use was approved by the University of Kentucky Institutional Review Board.

The cumulative quantity of drug collected in the receiver compartment was plotted as a function of time. The flux value for a given experiment was obtained from the slope of the steady state portion of the plot. Apparent permeability coefficient values were computed from Fick's First Law of diffusion:

$$\frac{1}{A}\left(\frac{dM}{dt}\right)=J_s=K_p\Delta C \quad (1)$$

where, J_s is the steady-state flux, M is the cumulative amount of drug permeating the skin, A is the area of the skin (0.95 cm^2), K_p is the effective permeability coefficient in cm/h, and ΔC is the difference in concentrations of NTX or prodrug in the donor and receiver compartment. Since sink conditions were maintained in the receiver compartment throughout the experiment, ΔC was approximated with the drug concentration in the donor compartment.

Drug disposition in the skin samples was measured at the completion of the 48 h experiment. The skin tissue was rinsed with filtered water and blotted with a paper towel. To remove the drug formulation adhering to the surface, the skin was tape-stripped twice using book tape (Scotch™, St. Paul, MN). The skin that was in contact with the drug was excised, minced with a scalpel, and placed in a pre-weighed vial. Drug was extracted from the skin by equilibrating with 10 mL of ACN in a shaking water bath overnight. Samples were analyzed by HPLC to determine NTX and NTX prodrug content and expressed as micromoles of drug per gram of wet tissue weight.

Chemical Stability of NTX Prodrugs in Buffer

The stability of NTX prodrugs in Hanks' buffer (pH 7.4) was examined using sub-saturated concentrations. Samples (6 mL) were distributed in screw-capped vials and placed in a water-bath at 32°C. One vial was removed immediately after the start of the experiment and other vials were removed at predetermined time intervals. Stability studies were conducted over 2 days with the N-monoalkyl carbamate prodrugs and over 14 days with N,N-dialkyl carbamate prodrugs. Drug was extracted from the buffer using solid phase extraction, and the samples were stored at −70°C until HPLC analysis. Percent of drug remaining (on a logarithmic scale) was plotted against time, to calculate pseudo-first order rate constants and half-lives of the prodrugs.

Plasma Hydrolysis of Prodrugs

Human plasma, stored at −20°C, was thawed at room temperature. Known amounts of the prodrug were added to the human plasma, vortexed and incubated at 37°C. Samples were withdrawn immediately after the start of the experiment and at regular time intervals thereafter and stored at −70°C until analysis. Study duration was 10 h for N-monoalkyl carbamate prodrugs and 48 h for the N,N-dialkyl carbamate prodrugs. A five-fold volume of ACN was added to precipitate protein, the solution was then vortexed and spun at 10,000 × g for 15 min. Supernatant was separated and evaporated under nitrogen at room temperature. The residue was reconstituted with ACN and then stored at ×70°C until analyzed by HPLC. A standard curve was prepared from the drug-spiked plasma samples that were processed by the same method. Percent of drug remaining (on a logarithmic scale) was plotted against time to calculate pseudo first order rate constants and half-lives of the prodrugs.

Stratum Corneum/Vehicle Partition Coefficient Studies

Human epidermis with the stratum corneum (SC) side facing up was incubated on filter papers soaked with 0.1% trypsin in 0.5% sodium bicarbonate solution in a petri dish at 37°C for 3 h. [21] The SC membrane was separated and dried in a vacuum desiccator. After 24 h, the SC was dipped in acetone for 20 sec to remove sebaceous lipids, and dried again.

Approximately 5 mg of SC was equilibrated with drug in 0.5 g of mineral oil at 32°C for 48 h. An aliquot of the mineral oil solution (10 μL) was withdrawn at the end of the study and

was diluted to 1 mL with ACN. The samples were then analyzed by HPLC. The amount of the drug in the SC was measured by subtracting the amount present in the mineral oil after equilibration from the initial drug concentration in the mineral oil. The partition coefficient value was expressed as concentration of prodrug in 1 g of SC to concentration of prodrug in 1 g of mineral oil.

RESULTS AND DISCUSSION

Four N-monoalkyl and three N,N-dialkyl carbamate prodrugs of NTX were synthesized by linking the phenolic hydroxyl group of NTX *via* a carbamoyl moiety containing straight-chain and branched N-alkyl groups. The structure of NTX and the prodrugs are shown in Figure 1.

Thermal Properties

Physicochemical characterization of these prodrugs, necessary for establishing quantitative-structure permeability relationships, included thermal parameters, such as melting points and heats of fusion that can be used to evaluate properties such as intermolecular cohesion, solubility, and thermodynamic activity.[14,22] All the NTX prodrugs, with the exception of the N,N-dimethyl carbamate prodrug, exhibited lower melting points than NTX, indicating that the addition of alkyl groups disrupts the intermolecular cohesion of NTX (Table I). These results are in agreement with earlier studies with carboxylate and carbonate prodrugs of NTX.[13,14] The melting points of all N-monoalkyl carbamate prodrugs were below 80°C (measured on a conventional melting point apparatus) suggesting that intermolecular cohesion was lowered to a greater extent for monoalkyl prodrugs compared to the N,N-dialkyl carbamates. The absence of endothermic peaks in DSC heating curves corroborates the low intermolecular cohesion of the N-monoalkyl carbamate prodrugs. The decrease in melting point with increasing chain length for the N-monoalkyl carbamate prodrugs (Table I) appears to be similar to trends observed earlier with straight chain carboxylate ester prodrugs of NTX.[14]

Solubility in Light Mineral Oil and in Buffer

The solubility of NTX and NTX carbamate prodrugs in light mineral oil and in Hanks' buffer are shown in Table II. The higher solubilities of the prodrugs in light mineral oil compared to parent NTX, except for the N,N-dimethyl carbamate prodrug, are consistent with their lower melting points. All prodrugs, except the ethyl carbamate prodrug, exhibited lower solubility in Hanks' buffer than parent NTX. The general decrease in aqueous solubilities of the prodrugs is likely due to the blocking of the phenolic hydroxyl group of NTX with the carbamate prodrug moieties, since this acidic hydroxyl group affords considerable aqueous solubility to the NTX molecule. The decrease in solubility of the N-monoalkyl carbamates in Hanks' buffer with increasing alkyl chain length is also consistent with previous observations on solubility of straight chain carboxylic ester and carbonate prodrugs of NTX.[13,14]

Maximum Flux from Light Mineral Oil

The flux values of NTX prodrugs were obtained from the terminal linear portion of the slope of cumulative amount of prodrug and NTX from prodrug vs. time. The data were plotted in NTX equivalents permeated over time. A representative permeation profile used to determine the steady-state flux of NTX from NTX, and of prodrug and bioconverted NTX from the prodrug, is shown in Figure 2. The mean flux values for NTX and its carbamate prodrugs are shown in Table II. It is evident from Table II that all N-monoalkyl carbamates exhibited higher fluxes than NTX itself, whereas the N,N-dialkyl carbamates exhibited similar or lower permeation than NTX. In order to minimize inter-subject and intra-subject variability associated with the use of three different sections of human skin from different donors, NTX was included as a control in each diffusion study. Thus, flux enhancement for each diffusion study with prodrug, defined as the ratio of NTX equivalent flux from prodrug to NTX control

flux, was calculated and is listed in Table II. The enhancement in flux appears to be quite reproducible for all the prodrugs. The flux enhancement for N-monoalkyl carbamates decreases slightly with increasing alkyl chain length and is consistent with similar trends observed in earlier studies of straight chain carboxylate ester prodrugs of NTX.[14] In contrast to the enhancement in flux from N-monoalkyl carbamate prodrugs, a decreased NTX equivalent flux was observed with N,N-dialkyl carbamate prodrugs.

Activity Coefficients

The thermodynamic activity coefficient of a drug is an important physicochemical property that can help to predict and explain skin partition coefficients and permeation across skin.[22] A higher activity coefficient corresponds with a greater permeation of drug through skin. Since no endothermic peaks were observed in the melting curves of the N-monoalkyl carbamates, their activity coefficient is most likely close to unity (Table I), and much higher than that for NTX. Activity coefficients of the N,N-dialkyl carbamates were lower than NTX. Pillai *et al.*[13] demonstrated a direct relationship between the flux of carbonate prodrugs of NTX and their thermodynamic activity coefficients. The relationship between activity and permeation of the carbamate prodrugs in this study appears to be similar and the lower melting NTX prodrugs showed the highest transdermal flux.

Permeability coefficients

The permeability coefficients of NTX and its carbamate prodrugs did not correlate with the observed flux and underscores the utility of J_{max} (maximum flux from a saturated solution) values when comparing transdermal drug delivery characteristics (Table II). It is also clear from the results in Table II that the solubilities of the prodrugs in light mineral oil and in Hanks' buffer do not correlate with flux values in a direct manner. It is likely that permeability coefficient calculations based on prodrug donor concentrations may not be entirely applicable since the carbamate prodrugs are expected to be bioconverted to the parent drug *via* hydrolytic cleavage by skin esterase enzymes.[23,24] It has also been reported that maximal flux is a more appropriate parameter than permeability, since it represents the amount penetrating the skin, and does not include solubility factors.[25]

Factors Affecting Maximal Flux of Carbamate Prodrugs

The flux of drug substrates across human skin is determined by both diffusion and metabolism in viable tissues. Both factors need to be considered with prodrugs since bioconversion of the prodrug to the parent drug is essential for therapeutic action. Thus, both mass transport and metabolism influence overall flux of drug. Several physical models that incorporate simultaneous diffusion and metabolism have been proposed in the literature.[26-31] However, stratum corneum permeability is the primary factor that determines prodrug and parent drug concentrations in the dermis. It is also clear from the models presented that for prodrugs with similar permeability across stratum corneum the levels and distribution of skin esterases determine total flux, since enzymatic bioconversion of the prodrug in the viable layers is also important.[27,28]

Bioconversion of Prodrugs

The disposition of the prodrugs in skin at 48 h indicates a 0–33% bioconversion to NTX during permeation (Figure 3). N-Monoalkyl carbamate prodrugs generated higher percentages of NTX than N,N-dialkyl carbamate prodrugs. The bioconversion rates of prodrugs in skin can influence the flux of the drugs.[32,33] For example, a prodrug that undergoes conversion in skin may increase the flux by a factor of $\sqrt{k/D}$ where 'k' is a metabolic rate constant and 'D' is the diffusivity of the drug in the viable tissue.[28] Therefore, faster metabolic rate constants can increase the flux of the prodrug by creating higher concentration gradients for the prodrug

across the skin.[33] An ideal prodrug should exhibit excellent chemical stability with fast enzymatic conversion in the body. Carbamate prodrugs may sometimes be preferred to ester prodrugs in dosage forms due to the potential for carbamates to be generally more stable to chemical hydrolysis. N-Monoalkyl carbamate prodrugs hydrolyzed faster in Hanks' buffer than did N,N-dialkyl prodrugs. The N,N-dialkyl carbamate prodrugs were very stable and did not undergo significant degradation over 14 days at 32°C (Table II). Prodrugs that are not completely converted to the parent drug during skin permeation should be detected in the systemic circulation. Plasma hydrolysis rates can also help predict the relative prodrug conversion rates to parent drug in the body. N,N-Dialkyl carbamate prodrugs were stable in plasma for 48 h at 37°C, whereas the N-monoalkyl carbamate prodrugs exhibited plasma half lives shorter than 2 h (Table II). Similar trends with carbamate ester prodrugs of entacapone have been reported in human serum.[16] Thus, monosubstituted N-alkyl carbamate prodrugs exhibited half-lives ranging from 1.9-2.7 h, whereas disubstituted N,N-dialkyl prodrugs did not release entacapone.[16] Previous studies with carbamate ester prodrugs have indicated that, in general, N,N-dialkyl prodrugs exhibit much lower enzymatic hydrolysis compared to N-alkyl prodrugs.[34-36] The higher stability of the N,N-dialkyl carbamate prodrugs suggests steric hindrance in the vicinity of the carbamate linkage as compared to the N-monoalkyl prodrugs.[19,37]

N,N-dialkyl and bulky N-monoalkyl carbamates have also been reported to be efficient inhibitors of hydrolytic esterases such as acetylcholinesterase and butylcholinesterase.[34,38-41] The effect of an N-alkyl group has been shown to profoundly affect affinity of carbamates for hydrolytic enzyme and resultant inhibitory action. In particular, increasing alkyl chain length from methyl to ethyl was found to dramatically decrease binding as well as potency of action.[41,42] The anomalous behavior with ethyl substituents has been ascribed to a disruption of the catalytic triad by the conformational restrictions and limited rotational freedom of the N-ethyl carbamates within the binding pocket of the enzyme.[38]

The lower extent of bioconversion of N,N-dialkyl carbamate prodrugs may contribute to the lower overall flux across skin compared to the N-monoalkyl carbamate prodrugs. Indeed, an excellent linear correlation between maximum flux of the carbamate prodrugs with their extent of bioconversion was evident ($r^2 = 0.91$; plot not shown). The correlation of flux with extent of bioconversion is consistent with physical models incorporating simultaneous diffusion and metabolism effects[27,28,31,43] as well as the results described in previous reports with naltrexone codrugs.[44-46] However, the lower flux from N,N-dialkyl carbamate prodrugs may not be due to lower bioconversion effects alone. Permeability of the N,N-dialkyl prodrugs across skin is also a major determinant of flux since the total amounts of intact prodrug found in skin and receiver at 48 h were significantly lower than the corresponding amounts for the N-monoalkyl prodrugs. Lower bioconversion alone would have led to greater amounts of prodrug in the receiver or in the systemic circulation. Hansen *et al*. reported plasma levels of intact disubstituted carbamate prodrugs of dopamine D-1 antagonists that were higher and eliminated more slowly (detected upto 12 h) than monosubstituted analogs (not detected after 2 h) following oral administration in dogs.[34] Interestingly, plasma levels of parent drug following oral administration of N-alkyl and N-dialkyl carbamate prodrugs of the presynaptic dopamine autoreceptor agonist (-)-3-(3-hydroxyphenyl)-N-propylpiperidine to rats indicate parallel behavior with the flux of the carbamate prodrugs across skin.[36] It is quite likely that the lower overall flux from N,N-dialkyl carbamate prodrugs is due to the significantly lower extent of partitioning of the prodrugs into skin from light mineral oil solutions compared to that of N-monoalkyl prodrugs.

Stratum Corneum/Vehicle Partition Coefficients

A comparison of the partition coefficients of select carbamate prodrugs between SC and mineral oil suggests that the significantly lower flux of NTX from N,N-dialkyl prodrugs relative to that from N-monoalkyl prodrugs may be attributed to the much lower partitioning of the former prodrugs into human skin. Thus, the N-monosubstituted ethyl and butyl carbamate prodrugs exhibited higher SC/vehicle partition coefficients (80.95 ± 7.25 and 93.90 ± 12.34, respectively) than the N,N-disubstituted dimethyl and diethyl carbamate prodrugs (16.48 ± 4.29 and 14.18 ± 1.00, respectively).

Permeability/Flux Models

A variety of quantitative structure-activity relationships to predict transdermal flux and permeability of drugs have been reported.[47-51] The simplest models to predict permeability across biological membranes are based on lipophilicity indicators such as octanol-water or hexadecane-water partition coefficients. The inclusion of other parameters such as molecular weight and hydrogen bonding has been shown to improve the predictive capabilities of the models. Models incorporating lipophilicity and molecular weight are, in general, quite successful in predicting the permeation of small molecules. The inability to predict permeability of bulkier molecules or of molecules with branched structures with such models suggested that other parameters of size, such as molecular volume, may be more appropriate than molecular weight. A majority of the predictive models assume homogeneity of the bilayer barrier properties of the stratum corneum and interpret their derivations based on bulk solubility diffusion theories across bilayers with uniform solvent-like properties. However, it has been shown that the permeability of solutes in biological membranes depend on both the lipid chain packing in the membrane[52,53] and the size of the solute.[54,55]

The steep dependence of permeation rates on permeant size has generally been ascribed to changes in diffusion within the membrane.[55] Anderson *et al*. have suggested that permeant size affects partitioning into bilayer membranes rather than diffusion, and that increased chain ordering within the membrane amplifies size selectivity.[53,56,57] The authors investigated the effects of lipid chain packing and permeant size and shape on permeability across lipid bilayers in gel and liquid crystalline dipalmitoylphosphatidylcholine (DPPC) bilayers using seven short-chain monocarboxylic acids (formic acid, acetic acid, propionic acid, butyric acid, valeric acid, isovaleric acid, and trimethylacetic acid) as permeants.[53] The experimental permeability coefficients were considerably lower than those predicted using a bulk solubility diffusion model wherein the bilayer membrane was represented by hexadecane. The natural logarithm of the permeability decrement factor, f, introduced to account for the effects of chain ordering, was found to correlate linearly with the inverse of the bilayer free surface area. The slope, which measures the sensitivity of the permeability coefficient of a given permeant to bilayer chain packing, exhibited an excellent linear correlation (r^2 = 0.94) with the minimum cross-sectional area of the permeant and a poor correlation (r^2 = 0.59) with molecular volume, suggesting that in the bilayer interior the permeants prefer to move with their long principal axis along the bilayer normal.[57,58] Other approaches that incorporate the heterogeneous nature of the stratum corneum bilayer barrier have also been reported.[59,60]

Evaluation of Models

The mean maximum flux values of the carbamate prodrugs (Table II) were fit to the Roberts and Sloan equation[51] as well as modifications incorporating the relative cross-sectional area of the carbamate head-groups or the relative cross-sectional area scaled by molecular weight (MW) in place of MW. The cross-sectional areas of the head groups of the N-monoalkyl and N,N-dialkyl carbamate prodrugs measured using SYBYL® 6.8.1 software **(Tripos Inc., St Louis, MO)** are listed in Table III. A relative cross-sectional area, normalized to the ethyl

prodrug value, was defined in order to obtain a dimensionless quantity that could be used in empirical predictive equations to describe experimentally obtained flux.

Model fitting and parameter estimations using the equations defined below were performed with nonlinear regression analyses using SigmaPlot 10.0 (SPSS, Chicago, IL). In addition to the Roberts and Sloan equation derived using the Potts-Guy approach[47] (Equation 2),

$$\text{Log } J_{max} = a + b \times \text{Log } S_{oil} + (1 - b) \times \text{Log } S_{aq} - c \times MW \quad (2)$$

the following equations were also examined:

$$\text{Log } J_{max} = a + b \times \text{Log } S_{oil} + (1 - b) \times \text{Log } S_{aq} - c \times \text{rel CS area} \quad (3)$$

$$\text{Log } J_{max} = a + b \times \text{Log } S_{oil} + (1 - b) \times \text{Log } S_{aq} - c \times MW \times \text{rel CS area} \quad (4)$$

where rel CS area or MW × rel CS area replace the MW term.An empirical modification of equations 2, 3, and 4, delinking the Log S_{oil} and Log S_{aq} terms,

$$\text{Log } J_{max} = a + b \times \text{Log } S_{oil} + c \times \text{Log } S_{aq} - d \times MW \quad (5)$$

$$\text{Log } J_{max} = a + b \times \text{Log } S_{oil} + c \times \text{Log } S_{aq} - d \times \text{rel CS area} \quad (6)$$

$$\text{Log } J_{max} = a + b \times \text{Log } S_{oil} + c \times \text{Log } S_{aq} - d \times MW \times \text{rel CS area} \quad (7)$$

as well as equations containing MW or cross-sectional area terms alone were also evaluated.

$$\text{Log } J_{max} = a - d \times MW \quad (8)$$

$$\text{Log } J_{max} = a - d \times \text{rel CS area} \quad (9)$$

$$\text{Log } J_{max} = a - d \times MW \times \text{rel CS area} \quad (10)$$

All regression fits were carried out with the constraints that the regression coefficients b, c, and d be positive.

The results of the regression fits to NTX carbamate flux data are shown in Table IV. Fits of flux data for the carbamate prodrugs using the Roberts-Sloan equation, an example of bulk solvent diffusion approaches, were quite poor suggesting that bulk partitioning-diffusion theories are inadequate when branched isomers with identical molecular weights (or molecular volumes) are involved. It is also evident that incorporation of either the relative cross-sectional area or the relative area scaled with molecular weight improves the fit to some extent. An

empirical equation delinking the constants for Log S_{oil} and Log S_{aq} (equations 5, 6, and 7) appears to provide superior fits, especially when relative cross-sectional area terms are used in place of MW. The regression coefficients b and c, and thus Log S_{oil} and Log S_{aq} terms, were, however, statistically insignificant. Thus, fits containing the relative cross-sectional area terms alone (equations 8 and 9) were only marginally different (Table IV). It is quite clear from the results in Table IV that equations containing MW are considerably less capable of predicting the flux of isomeric branched NTX carbamate prodrugs. The correlation of flux with the relative cross-sectional area of the carbamate head group suggests strongly that predicting the transport of a series of prodrugs may only require knowledge of the cross-sectional area of the molecule, regardless of the vehicle used. Recent publications clearly suggest the importance of the cross-sectional area of the molecule in determining passive transport of drugs across the blood brain barrier.[61,62] A reinterpretation of previous flux results for straight-chain ester and carbonate ester prodrugs in terms of relative cross-sectional areas will be undertaken to validate this approach.

CONCLUSIONS

The nature of N-substitution is critical to the design of a successful carbamate prodrug for skin permeation. Thus, N-monoalkyl carbamate prodrugs significantly enhanced skin permeation and exhibited rapid plasma hydrolysis rates, whereas N,N-dialkyl carbamate prodrugs did not enhance NTX permeation. The significantly lower flux of the N,N-dialkyl prodrugs appears to be primarily due to a much larger free bilayer area requirement as well as to lower enzymatic hydrolysis rates compared to the N-alkyl carbamate prodrugs. The N-monoalkyl carbamate prodrugs will be pursued in future studies.

ACKNOWLEDGMENTS

The authors thank the National Cancer Institute Cooperative Human Tissue Network (CHTN) for supplying the skin tissue. This project was funded by NIH grant R01DA13425.

REFERENCES

1. Volpicelli JR, Alterman AI, Hayashida M, O'Brien CP. Naltrexone in the treatment of alcohol dependence. Arch Gen Psychiatry 1992;49(11):876–880. [PubMed: 1345133]
2. Terenius L. Rational treatment of addiction. Curr Opin Chem Biol 1998;2(4):541–547. [PubMed: 9736929]
3. PDR Generics. Vol. 2nd ed. Medical Economics; New Jersey: 1996. p. 2229-2233.
4. Rothenberg JL, Sullivan MA, Church SH, Seracini A, Collins E, Kleber HD, Nunes EV. Behavioral naltrexone therapy: an integrated treatment for opiate dependence. J Subst Abuse Treat 2002;23(4): 351–360. [PubMed: 12495797]
5. Volpicelli JR, Rhines KC, Rhines JS, Volpicelli LA, Alterman AI, O'Brien CP. Naltrexone and alcohol dependence. Role of subject compliance. Arch Gen Psychiatry 1997;54(8):737–742. [PubMed: 9283509]
6. Kranzler HR, Modesto-Lowe V, Van Kirk J. Naltrexone vs. nefazodone for treatment of alcohol dependence. A placebo-controlled trial. Neuropsychopharmacology 2000;22(5):493–503. [PubMed: 10731624]
7. Kydonieus, AF. Transdermal delivery of drugs. Kydonieus, AF.; Berner, B., editors. CRC Press; Boca Raton, FL: 1987.
8. Chen, YL.; Chun, LL.; Enscore, DJ. Transdermal therapeutic systems for the administration of naloxone, naltrexone, and nalbuphine. US Patent. # 4,573,995. 1986.
9. Vigroux A, Bergon M, Zedde C. Cyclization-activated prodrugs: N-(substituted 2-hydroxyphenyl and 2-hydroxypropyl)carbamates based on ring-opened derivatives of active benzoxazolones and oxazolidinones as mutual prodrugs of acetaminophen. J Med Chem 1995;38(20):3983–3994. [PubMed: 7562932]

10. Hussain MA, Aungst BJ, Koval CA, Shefter E. Improved buccal delivery of opioid analgesics and antagonists with bitterless prodrugs. Pharm Res 1988;5(9):615–618. [PubMed: 3247326]
11. Hussain MA, Koval CA, Myers MJ, Shami EG, Shefter E. Improvement of the oral bioavailability of naltrexone in dogs: a prodrug approach. J Pharm Sci 1987;76(5):356–358. [PubMed: 3656096]
12. Vlieghe P, Bihel F, Clerc T, Pannecouque C, Witvrouw M, De Clercq E, Salles JP, Chermann JC, Kraus JL. New 3′-azido-3′-deoxythymidin-5′-yl O-(omega-hydroxyalkyl) carbonate prodrugs: synthesis and anti-HIV evaluation. J Med Chem 2001;44(5):777–786. [PubMed: 11262088]
13. Pillai O, Hamad MO, Crooks PA, Stinchcomb AL. Physicochemical evaluation, in vitro human skin diffusion, and concurrent biotransformation of 3-O-alkyl carbonate prodrugs of naltrexone. Pharm Res 2004;21(7):1146–1152. [PubMed: 15290853]
14. Stinchcomb AL, Swaan PW, Ekabo O, Harris KK, Browe J, Hammell DC, Cooperman TA, Pearsall M. Straight-chain naltrexone ester prodrugs: diffusion and concurrent esterase biotransformation in human skin. J Pharm Sci 2002;91(12):2571–2578. [PubMed: 12434400]
15. Alexander J, Fromtling RA, Bland JA, Pelak BA, Gilfillan EC. (Acyloxy)alkyl carbamate prodrugs of norfloxacin. J Med Chem 1991;34(1):78–81. [PubMed: 1992156]
16. Savolainen J, Leppanen J, Forsberg M, Taipale H, Nevalainen T, Huuskonen J, Gynther J, Mannisto PT, Jarvinen T. Synthesis and in vitro/in vivo evaluation of novel oral N-alkyl- and N,N-dialkyl-carbamate esters of entacapone. Life Sci 2000;67(2):205–216. [PubMed: 10901288]
17. Sun X, Zeckner DJ, Current WL, Boyer R, McMillian C, Yumibe N, Chen SH. N-acyloxymethyl carbamate linked prodrugs of pseudomycins are novel antifungal agents. Bioorg Med Chem Lett 2001;11(14):1875–1879. [PubMed: 11459651]
18. Alexander J, Cargill R, Michelson SR, Schwam H. (Acyloxy)alkyl carbamates as novel bioreversible prodrugs for amines: increased permeation through biological membranes. J Med Chem 1988;31(2): 318–322. [PubMed: 2892933]
19. Carvalho E, Francisco AP, Iley J, Rosa E. Triazene drug metabolites. Part 17: Synthesis and plasma hydrolysis of acyloxymethyl carbamate derivatives of antitumour triazenes. Bioorg Med Chem 2000;8(7):1719–1725. [PubMed: 10976519]
20. Fort JJ, Shao ZZ, Mitra AK. Transport and degradation characteristics of methotrexate dialkyl ester prodrugs across tape-stripped hairless mouse skin. Int J Pharm 1993;100:233–239.
21. Kligman AM, Christophers E. Preparation of isolated sheets of human stratum corneum. Arch Dermatol 1963;88:702–705. [PubMed: 14071437]
22. Stinchcomb AL, Dua R, Paliwal A, Woodard RW, Flynn GL. A solubility and related physicochemical property comparison of buprenorphine and its 3-alkyl esters. Pharm Res 1995;12(10):1526–1529. [PubMed: 8584493]
23. Hewitt PG, Perkins J, Hotchkiss SA. Metabolism of fluroxypyr, fluroxypyr methyl ester, and the herbicide fluroxypyr methylheptyl ester. II: in rat skin homogenates. Drug Metab Dispos 2000;28 (7):755–759. [PubMed: 10859148]
24. Hewitt PG, Perkins J, Hotchkiss SA. Metabolism of fluroxypyr, fluroxypyr methyl ester, and the herbicide fluroxypyr methylheptyl ester. I: during percutaneous absorption through fresh rat and human skin in vitro. Drug Metab Dispos 2000;28(7):748–754. [PubMed: 10859147]
25. Magnusson BM, Anissimov YG, Cross SE, Roberts MS. Molecular size as the main determinant of solute maximum flux across the skin. J Invest Dermatol 2004;122(4):993–999. [PubMed: 15102090]
26. Stehle RG, Ho NF, Barsuhn CL, Stefanski KJ. Local topical delivery of drugs: a model incorporating simultaneous diffusion and metabolic interconversion between drug and a single metabolite in the skin. J Theor Biol 1989;138(1):1–15. [PubMed: 2626062]
27. Yu CD, Fox JL, Ho NF, Higuchi WI. Physical model evaluation of topical prodrug delivery-simultaneous transport and bioconversion of vidarabine-5′-valerate II: parameter determinations. J Pharm Sci 1979;68(11):1347–1357. [PubMed: 512881]
28. Yu CD, Fox JL, Ho NF, Higuchi WI. Physical model evaluation of topical prodrug delivery-simultaneous transport and bioconversion of vidarabine-5′-valerate I: physical model development. J Pharm Sci 1979;68(11):1341–1346. [PubMed: 512880]
29. Guzek DB, Kennedy AH, McNeill SC, Wakshull E, Potts RO. Transdermal drug transport and metabolism. I. comparison of in vitro and in vivo results. Pharm Res 1989;6(1):33–39. [PubMed: 2717514]

30. Potts RO, McNeill SC, Desbonnet CR, Wakshull E. Transdermal drug transport and metabolism. II. The role of competing kinetic events. Pharm Res 1989;6(2):119–124. [PubMed: 2762211]

31. Fox JL, Cheng-Dur Y, Higuchi WI, Ho NFH. General physical model for simultaneous diffusion and metabolism in biological membranes. The computational approach for the steady-state case. Int J Pharm 1979;2:41–57.

32. Bando H, Mohri S, Yamashita F, Takakura Y, Hashida M. Effects of skin metabolism on percutaneous penetration of lipophilic drugs. J Pharm Sci 1997;86(6):759–761. [PubMed: 9188062]

33. Hammell DC, Hamad M, Vaddi HK, Crooks PA, Stinchcomb AL. A duplex “Gemini” prodrug of naltrexone for transdermal delivery. J Control Release 2004;97(2):283–290. [PubMed: 15196755]

34. Hansen KT, Jansen JA, Mengel H, Christensen JV, Bundgaard H. Enhanced bioavailability of a new class of dopamine D-1 antagonists following oral administration of their carbamic acid ester prodrugs to dogs. Int J Pharm 1992;79:205–212.

35. Olsson OAT, Svensson LA. New lipophilic terbutaline ester prodrugs with long effect duration. Pharm Res 1984;1:19–23.

36. Thorberg SO, Berg S, Lundstrom J, Pettersson B, Wijkstrom A, Sanchez D, Lindberg P, Nilsson JL. Carbamate ester derivatives as potential prodrugs of the presynaptic dopamine autoreceptor agonist (-)-3-(3-hydroxyphenyl)-N-propylpiperidine. J Med Chem 1987;30(11):2008–2012. [PubMed: 3669008]

37. Safadi M, Oliyai R, Stella VJ. Phosphoryloxymethyl carbamates and carbonates--novel water-soluble prodrugs for amines and hindered alcohols. Pharm Res 1993;10(9):1350–1355. [PubMed: 8234176]

38. Bar-On P, Millard CB, Harel M, Dvir H, Enz A, Sussman JL, Silman I. Kinetic and structural studies on the interaction of cholinesterases with the anti-Alzheimer drug rivastigmine. Biochemistry 2002;41(11):3555–3564. [PubMed: 11888271]

39. Bartolucci C, Siotto M, Ghidini E, Amari G, Bolzoni PT, Racchi M, Villetti G, Delcanale M, Lamba D. Structural determinants of Torpedo californica acetylcholinesterase inhibition by the novel and orally active carbamate based anti-alzheimer drug ganstigmine (CHF-2819). J Med Chem 2006;49 (17):5051–5058. [PubMed: 16913695]

40. Groner E, Ashani Y, Schorer-Apelbaum D, Sterling J, Herzig Y, Weinstock M. The kinetics of inhibition of human acetylcholinesterase and butyrylcholinesterase by two series of novel carbamates. Mol Pharmacol 2007;71(6):1610–1617. [PubMed: 17347320]

41. Bolognesi ML, Bartolini M, Cavalli A, Andrisano V, Rosini M, Minarini A, Melchiorre C. Design, synthesis, and biological evaluation of conformationally restricted rivastigmine analogues. J Med Chem 2004;47(24):5945–5952. [PubMed: 15537349]

42. Sterling J, Herzig Y, Goren T, Finkelstein N, Lerner D, Goldenberg W, Miskolczi I, Molnar S, Rantal F, Tamas T, Toth G, Zagyva A, Zekany A, Finberg J, Lavian G, Gross A, Friedman R, Razin M, Huang W, Krais B, Chorev M, Youdim MB, Weinstock M. Novel dual inhibitors of AChE and MAO derived from hydroxy aminoindan and phenethylamine as potential treatment for Alzheimer’s disease. J Med Chem 2002;45(24):5260–5279. [PubMed: 12431053]

43. Kiptoo, PK. PhD Thesis. Department of Pharmaceutical Sciences, University of Kentucky College of Pharmacy, University of Kentucky; 2007. Transdermal delivery of naltrexone and its active metabolite, 6-beta-naltrexol, via novel tripartate codrugs linked to bupropion and hydroxybupropion; p. 199

44. Hamad MO, Kiptoo PK, Stinchcomb AL, Crooks PA. Synthesis and hydrolytic behavior of two novel tripartate codrugs of naltrexone and 6beta-naltrexol with hydroxybupropion as potential alcohol abuse and smoking cessation agents. Bioorg Med Chem 2006;14(20):7051–7061. [PubMed: 16798000]

45. Kiptoo PK, Hamad MO, Crooks PA, Stinchcomb AL. Enhancement of transdermal delivery of 6-beta-naltrexol via a codrug linked to hydroxybupropion. J Control Release 2006;113(2):137–145. [PubMed: 16750868]

46. Kiptoo PK, Paudel KS, Hammell DC, Hamad MO, Crooks PA, Stinchcomb AL. In vivo evaluation of a transdermal codrug of 6-beta-naltrexol linked to hydroxybupropion in hairless guinea pigs. Eur J Pharm Sci 2008;33(45):371–379. [PubMed: 18321686]

47. Potts RO, Guy RH. Predicting skin permeability. Pharm Res 1992;9(5):663–669. [PubMed: 1608900]

48. Potts RO, Guy RH. A predictive algorithm for skin permeability: the effects of molecular size and hydrogen bond activity. Pharm Res 1995;12(11):1628–1633. [PubMed: 8592661]

49. Pugh WJ, Roberts MS, Hadgraft J. Epidermal permeability-penetrant structure relationship: 3. the effect of hydrogen bonding interactions and molecular size on diffusion across the stratum corneum. Int J Pharm 1996;138:149–165.

50. Roberts MS, Pugh WJ, Hadgraft J, Watkinson AC. Epidermal permeability-penetrant structure relationships: 1. an analysis of methods of predicting penetration of monofunctional solutes from aqueous solutions. Int J Pharm 1995;126:219–233.

51. Roberts WJ, Sloan KB. Prediction of transdermal flux of prodrugs of 5-fluorouracil, theophylline, and 6-mercaptopurine with a series/parallel model. J Pharm Sci 2000;89(11):1415–1431. [PubMed: 11015687]

52. Xiang TX, Anderson BD. Phospholipid surface density determines the partitioning and permeability of acetic acid in DMPC:cholesterol bilayers. J Membr Biol 1995;148(2):157–167. [PubMed: 8606364]

53. Xiang TX, Anderson BD. Permeability of acetic acid across gel and liquid-crystalline lipid bilayers conforms to free-surface-area theory. Biophys J 1997;72(1):223–237. [PubMed: 8994607]

54. Xiang TX, Anderson BD. Substituent contributions to the transport of substituted p-toluic acids across lipid bilayer membranes. J Pharm Sci 1994;83(10):1511–1518. [PubMed: 7884677]

55. Walter A, Gutknecht J. Permeability of small nonelectrolytes through lipid bilayer membranes. J Membr Biol 1986;90(3):207–217. [PubMed: 3735402]

56. Xiang TX, Anderson BD. Influence of chain ordering on the selectivity of dipalmitoylphosphatidylcholine bilayer membranes for permeant size and shape. Biophys J 1998;75 (6):2658–2671. [PubMed: 9826590]

57. Xiang TX, Anderson BD. The relationship between permeant size and permeability in lipid bilayer membranes. J Membr Biol 1994;140(2):111–122. [PubMed: 7932645]

58. Xiang TX, Anderson BD. Molecular distributions in interphases: statistical mechanical theory combined with molecular dynamics simulation of a model lipid bilayer. Biophys J 1994;66(3 Pt 1): 561–572. [PubMed: 8011890]

59. Bemporad D, Luttmann C, Essex JW. Computer simulation of small molecule permeation across a lipid bilayer: dependence on bilayer properties and solute volume, size, and cross-sectional area. Biophys J 2004;87(1):1–13. [PubMed: 15240439]

60. Mitragotri S. A theoretical analysis of permeation of small hydrophobic solutes across the stratum corneum based on Scaled Particle Theory. J Pharm Sci 2002;91(3):744–752. [PubMed: 11920759]

61. Gerebtzoff G, Seelig A. In silico prediction of blood-brain barrier permeation using the calculated molecular cross-sectional area as main parameter. J Chem Inf Model 2006;46(6):2638–2650. [PubMed: 17125204]

62. Seelig A. The role of size and charge for blood-brain barrier permeation of drugs and fatty acids. J Mol Neurosci 2007;33(1):32–41. [PubMed: 17901543]

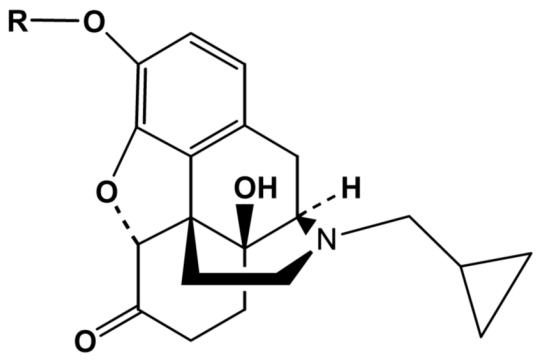

DRUG	R-GROUP
NTX	-H
N-monoalkyl prodrugs	
ETHYL	$-CONHCH_2CH_3$
PROPYL	$-CONH(CH_2)_2CH_3$
BUTYL	$-CONH(CH_2)_3CH_3$
PENTYL	$-CONH(CH_2)_4CH_3$
N,N-dialkyl prodrugs	
DIMETHYL	$-CON(CH_3)_2$
DIETHYL	$-CON(CH_2CH_3)_2$
DIISOPROPYL	$-CON(CH(CH_3)_2)_2$

Figure 1.
Chemical structure of NTX and its 3-O-carbamate prodrugs

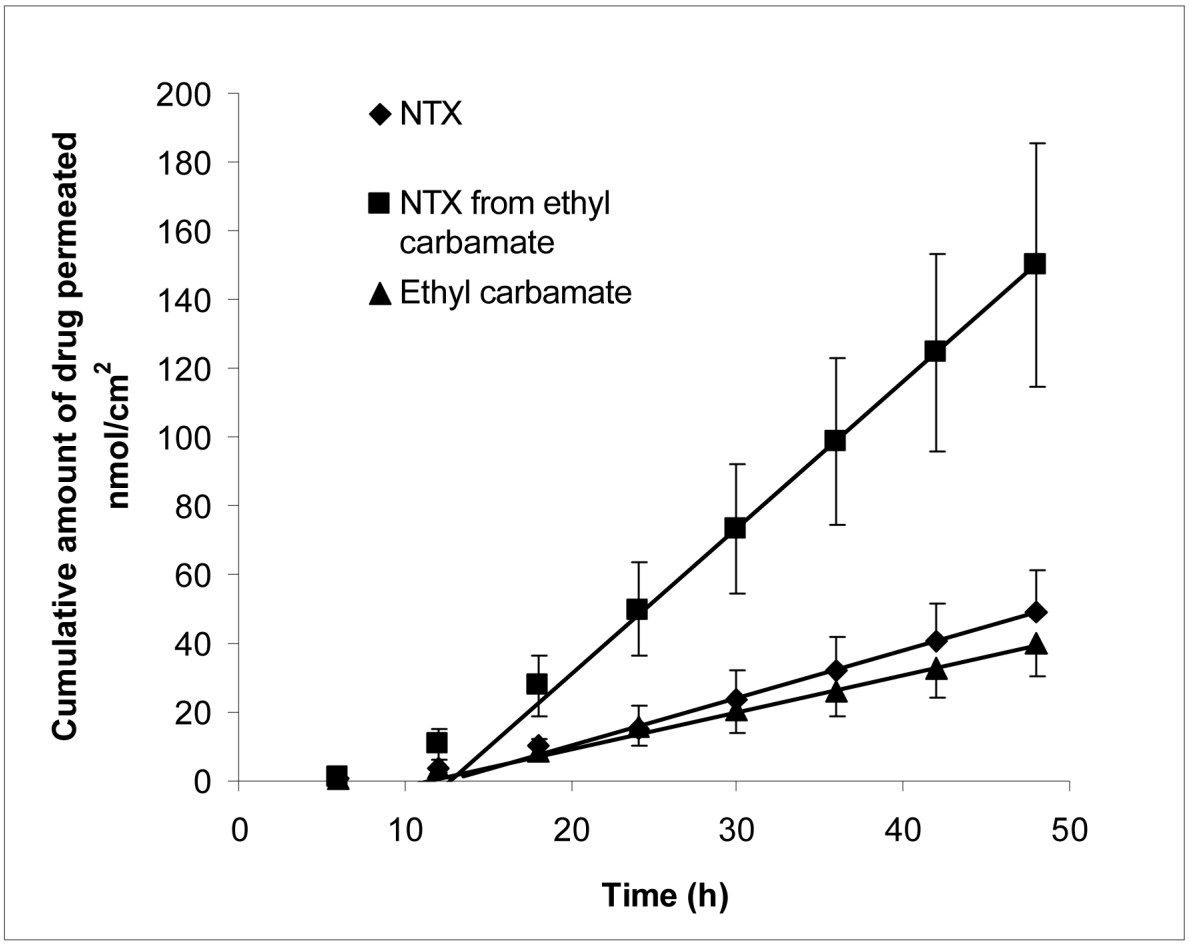

Figure 2.
Representative permeation profiles of NTX from NTX, and NTX and N-ethyl carbamate prodrug from N-ethyl carbamate, following application of saturated solutions to human skin at 32°C. Data expressed as mean ± SD (n = 3 for NTX and n = 4 for prodrug).

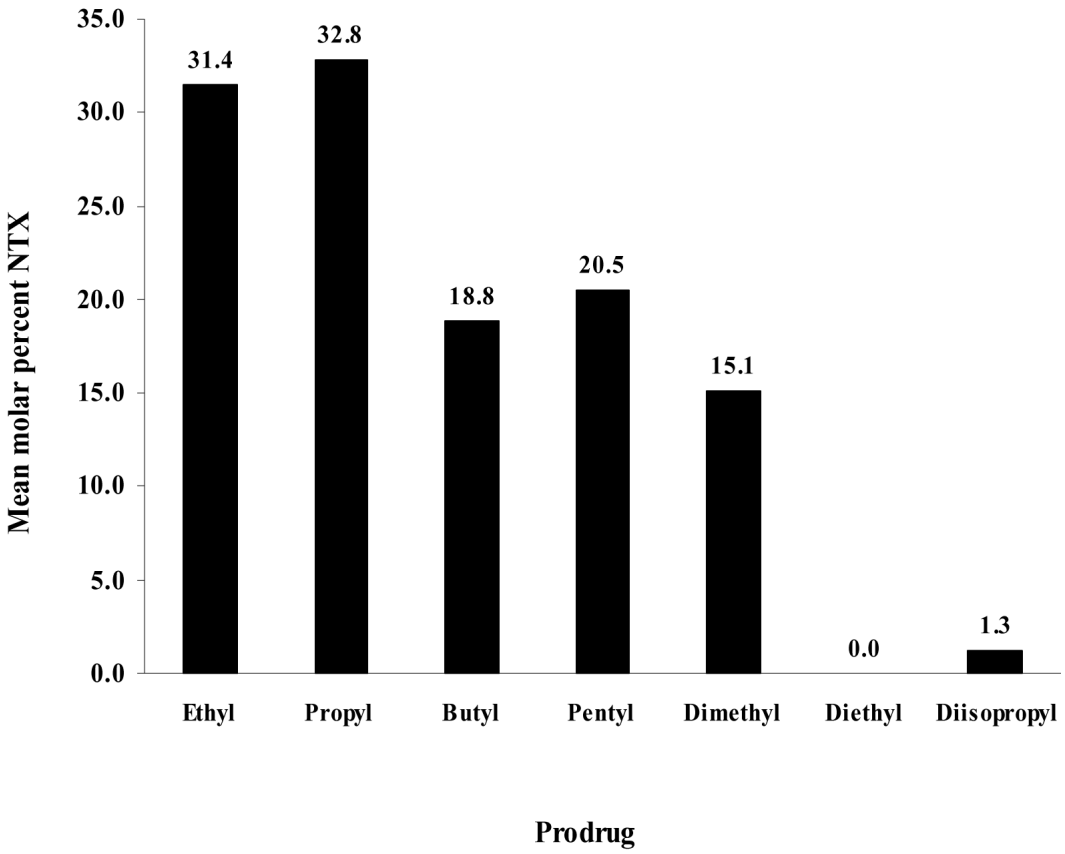

Figure 3.

Drug disposition in human skin at 48 h in permeation experiments with saturated solutions of drug or prodrug in light mineral oil. Data represents the mean molar percentage of regenerated NTX to total drug extracted from the skin.

Table I

Thermal properties of 3-O-carbamate NTX prodrugs.

DRUG/PRODRUG	MW	MP (°C)	Activity coefficient [a] at 25°C	Heats of fusion (kJ/mol)
NTX	341	174-176	0.14	14.75
N-ETHYL	412	78-80	--	ND[b]
N-PROPYL	425	75-77	--	ND
N-BUTYL	440	68-70	--	ND
N-PENTYL	453	65-67	--	ND
N,N-DIMETHYL	412	206-208	0.03	22.01
N,N-DIETHYL	440	146-147	0.08	21.56
N,N-DIISOPROPYL	468	147-149	0.09	19.95

where a_2 is thermodynamic activity, R is gas constant, T is room temperature, T_f is the fusion temperature and ΔH_f is heat of fusion (From J. H. Hildebrand and R. L. Scott).[38]

[a] Calculated from $\ln a_2 = \frac{-\Delta H_f}{RT}\left(\frac{T_f - T}{T_f}\right)$;

[b] Not detected

Table II

Solubility in oil and aqueous media, mean maximum flux, flux enhancement, permeability, and stability of NTX and its 3-O-carbamate prodrugs.

Drug/Prodrug	Solubility in light mineral oil[a] (mM)	Solubility in Hanks' buffer[a] (mM)	TEWL[a] ($g/m^2/h$)	Mean maximum flux from mineral oil[a] ($nmol/cm^2/h$)	Flux enhancement[a]	Permeability coefficient from mineral oil ($Kp \times 10^4$) cm/h	Plasma half-life (h)	Half-life in Hanks' buffer (h)
NTX	0.24 ± 0.02	6.18 ± 0.50	3.56 ± 2.07	3.68 ± 2.37		153	na	na
N-ETHYL	1.01 ± 0.09	14.19 ± 0.25	3.84 ± 2.34	15.53 ± 11.26	3.17 ± 0.31	153	1.45	9.35
N-PROPYL	0.96 ± 0.13	3.05 ± 0.09	3.91 ± 2.07	17.44 ± 11.16	3.23 ± 0.73	182	0.85	10.47
N-BUTYL	1.86 ± 0.11	2.63 ± 0.15	3.32 ± 1.21	7.99 ± 6.22	3.06 ± 0.65	43	1.49	11.55
N-PENTYL	0.52 ± 0.01	0.37 ± 0.02	3.53 ± 3.22	5.16 ± 3.34	2.10 ± 0.17	99	0.67	13.17
N,N-DIMETHYL	0.20 ± 0.00	3.00 ± 0.05	3.79 ± 1.60	2.94 ± 0.87	1.00 ± 0.59	147	ST[b]	ST
N,N-DIETHYL	1.29 ± 0.03	1.18 ± 0.03	4.55 ± 2.28	2.23 ± 2.03	0.58 ± 0.40	17	ST	ST
N,N-DIISOPROPYL	0.71 ± 0.01	0.87 ± 0.01	3.39 ± 3.01	1.51 ± 0.45	0.84 ± 0.53	21	ST	ST

na = not applicable

[a] Values expressed as mean ± SD

[b] ST: Stable = no significant degradation observed over duration of experiment

Table III

Relative cross-sectional area of head groups of N-monoalkyl and N,N-dialkyl 3-O-carbamate prodrugs of NTX

Prodrug	Relative cross-sectional area (rel CS area)	MW	MW × rel CS area
N-ETHYL	1.00	412	412.00
N-PROPYL	1.41	425	597.55
N-BUTYL	1.38	440	607.25
N-PENTYL	1.74	453	789.56
N,N-DIMETHYL	1.91	412	786.58
N,N-DIETHYL	2.47	440	1085.81
N,N-DIISOPROPYL	2.82	468	1320.69

Table IV

Non-linear regression analyses fit parameters

Equation	r^2	a	b	c	d
$\text{Log } J_{max} = a + b \times \text{Log } S_{oil} + (1\text{-}b) \times \text{Log } S_{aq} - c \times MW$	0.477	5.213 ± 6.385*	0.816 ± 0.538*	0.010 ± 0.014*	-
$\text{Log } J_{max} = a + b \times \text{Log } S_{oil} + (1\text{-}b) \times \text{Log } S_{aq} - c \times \text{rel CS area}$	0.676	1.395 ± 0.451**	0.695 ± 0.244**	0.380 ± 0.209*	-
$\text{Log } J_{max} = a + b \times \text{Log } S_{oil} + (1\text{-}b) \times \text{Log } S_{aq} - c \times MW \times \text{rel CS area}$	0.677	1.370 ± 0.436**	0.729 ± 0.252**	0.0008 ± 0.0004*	-
$\text{Log } J_{max} = a + b \times \text{Log } S_{oil} + c \times \text{Log } S_{aq} - d \times MW$	0.538	6.523 ± 6.259*	0.629 ± 0.617*	0.000 ± 0.490*	0.0132 ± 0.0140*
$\text{Log } J_{max} = a + b \times \text{Log } S_{oil} + c \times \text{Log } S_{aq} - d \times \text{rel CS area}$	0.899	1.800 ± 0.302**	0.209 ± 0.245*	0.000 ± 0.161*	0.5812 ± 0.1468**
$\text{Log } J_{max} = a + b \times \text{Log } S_{oil} + c \times \text{Log } S_{aq} - d \times MW \times \text{rel CS area}$	0.889	1.693 ± 0.338**	0.272 ± 0.260*	0.000 ± 0.218*	0.0012 ± 0.0004**
$\text{Log } J_{max} = a - d \times MW$	0.319	5.582 ± 3.180*	-	-	0.0112 ± 0.0073*
$\text{Log } J_{max} = a - d \times \text{rel CS area}$	0.875	1.813 ± 0.194***	-	-	0.6010 ± 0.1016**
$\text{Log } J_{max} = a - d \times MW \times \text{rel CS area}$	0.844	1.694 ± 0.199***	-	-	0.0012 ± 0.0002***

* p-value > 0.1

** p-value < 0.05

*** p-value < 0.01